Copyright European Association for Signal Processing, 2010, published in the proceedings of the third international EURASIP Workshop on RFID Technology, Sept. 2010

Direction of Arrival Estimation by Phased Arrays in RFID

Christoph Angerer, Robert Langwieser and Markus Rupp
Institute of Communications and Radio-Frequency Engineering
Vienna University of Technology, Austria
Email: {cangerer, rlang, mrupp}@nt.tuwien.ac.at

***Abstract* - In this paper we propose a direction of arrival estimation for a dual receive antenna RFID reader. In a strong line of sight environment, the phase shift on the elements of a receive array of the tag signal is utilised to estimate the direction of arrival of the tag. In RFID however, receive signals are impaired by a strong carrier leakage. The receive signal composition at each individual receive antenna is modeled, and based on that model, the phase shift determination is presented. The proposed receiver is implemented on an FPGA of an RFID rapid prototyping environment. Details about its implementation are given, and it is shown in an experimental evaluation by measurement, that the root of the averaged squared error over several position of the direction of arrival estimation is 3.3° with two antennas.**

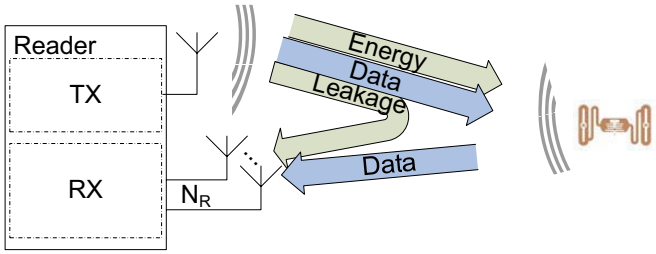

Figure 1: Communication between an RFID reader with multiple RX antennas and an RFID tag.

I. Introduction

Radio Frequency Identification (RFID) is in general employed for applications requiring identification and tracking of goods. Apart from these major purposes of RFID technology however, an additional information on localisation has recently attracted interest. While localisation has been proposed for active RFID before, we concentrate on passive UHF RFID, which has only very recently demonstrated to be feasible. Our approach employs two receive antennas for Direction of Arrival (DOA) estimation in low fading environments. While work by Kim et al. [1] estimate the direction of arrival by tracking the receive signal strength of two directional antennas depending on their orientation, the phase difference at distinct array elements is considered for direction of arrival estimation in this work. Additionally, several authors, for instance [2, 3] propose to install multiple readers and apply reader-to-tag distance estimation to localise an RFID tag. Similarily, a mobile RFID reader determines its own location by means of positioning tags at reference locations [4]. Other authors [5–7] propose to apply smart antennas to estimate the DOA and provide a theoretical analysis of the performance, while this paper also shows experimental results. Salonen et al. [8] show a phased array realisation for blindly scanning an area with a beam. Very recently, Nikitin et al. [9] published a comparison of different techniques of DOA estimation by utilising a phase difference. They propose to exploit a phase difference of a) multiple consecutive measurements of a moving tag (time domain), b) multiple consecutive measurements of a static tag with different carrier frequencies (frequency domain), and c) multiple receive antennas (spatial domain). While the spatial domain approach in their paper is of conceptual nature, we also show experimental results on this topic in this paper. Furthermore, Hekimian et al. [10] propose a DOA estimation in active RFID systems by combining two RFID reader modules. Both modules are synchronised by applying an external clock. As they use active RFID, they also need to compensate the carrier offset after downconversion. Their paper shows excellent experimental results. In contrast to their paper we establishes a DOA estimation for passive RFID. Additionally, Chia et al. [11, 12] show a solution for beam steering for RFID readers, by delaying the carrier synthesiser signals for different paths. Reader to tag distance estimation by means of a multi frequency continuous wave radar approach is for example shown in [13].

The paper is structured as follows: The next section introduces a model of signal constellations at multiple receive antennas of an RFID reader. Based on that model, we propose our DOA estimation algorithm in Section III. The following Section IV. treats the implementation of the receiver on a rapid prototyping platform, while Section V. presents measurement results of the DOA estimation in a low fading environment.

II. Model of signal constellations at a multiple receive antenna reader

Figure 1 shows the basic communication between a tag and a reader receiver with N_R antennas. Passive tags are supplied with energy by the RFID reader in form of a continuous carrier transmission, including time intervals of uplink communication. This continuous carrier transmission also leaks into the i'th receive antenna ($i \in 1 \dots N_R$):

$$s_i^{leak}(t) = |L_i| \sin(\omega_c t + \varphi_i^{leak}). \tag{1}$$

Here, φ_i^{leak} is the phase shift, which results from the propagation delay between the transmit and the receive path i. The amplitude $|L_i|$ of the leakage depends on the transmitter to receiver decoupling [14, 15].

The uplink communication applies backscatter modulation. During times the tag is not communicating, the input impedance of the tag is matched to the antenna impedance for maximum energy absorption. During communication cycles, the tag backscatters energy by switching its input impedance between the matched state and an unmatched state. This backscattered signal at the tag is given by:

$$s_{tag}(t) = a(t)\sqrt{|\Delta\sigma|}|h^f| \sin(\omega_c t + \varphi^f + \varphi^{\Delta\sigma}). \tag{2}$$

Here $|h^f|$ and φ^f denote the forward channel attenuation and phase shift. The modulation signal $a(t)$ switches between the matched and the unmatched state of the tag and realises an on-off keying ($a(t) \in \{0, 1\}$). The term $\varphi^{\Delta\sigma}$ describes the phase shift introduced by the tag modulation, while $|\Delta\sigma|$ is the normalised differential radar cross section as described by Nikitin et al. [16], which basically describes the modulation efficiency:

$$|\Delta\sigma| = |\rho_r - \rho_a|^2, \tag{3}$$

where ρ_r and ρ_a are the complex reflection coefficients for the tag's reflect and absorb state, respectively.

At the reader receive antenna i the tag signal adds with the carrier leakage:

$$\begin{aligned} s_i^{pb}(t) = |h_i^b|\sqrt{|\Delta\sigma|}|h^f|a(t) \sin(\omega_c t + \varphi^f + \varphi_i^b + \varphi^{\Delta\sigma}) \\ +|L_i| \sin(\omega_c t + \varphi_i^{leak}) + n_i^{pb}. \end{aligned} \tag{4}$$

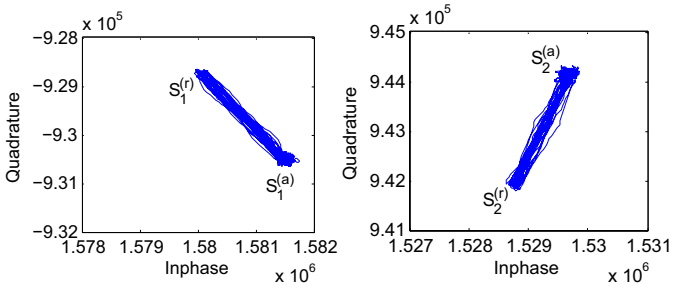

(a) Antenna 1 (b) Antenna 2

Figure 2: Tag response in baseband: inphase and quadrature constellations on both antennas. The offset from the origin results from the carrier leakage (tag absorb state $S_i^{(a)}$).

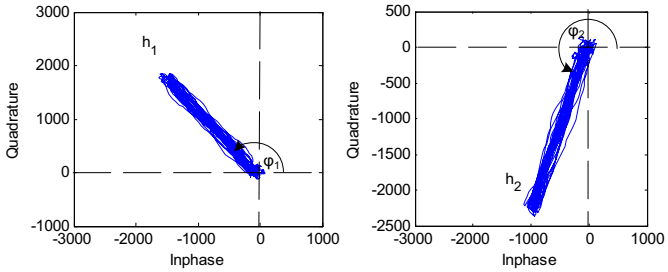

(a) Antenna 1 (b) Antenna 2

Figure 3: Tag response in baseband with removed carrier leakage: inphase and quadrature constellations on both RX branches. The phase shifts φ_i determine the DOA of the tag receive signal.

The terms $|h_i^b|$ and φ_i^b denote the backward channel attenuations and phase shifts from the tag to the i'th reader receive antenna. It is worth mentioning, that the signal components from the tag at the different receive antennas only differ in the backward channel attenuation $|h_i^b|$ and phase shift φ_i^b.

A downconversion without any frequency offset is readily possible at each antenna, as only a single frequency source (the oscillator in the transmitter of the reader) exists in the system. The complex-valued baseband signal at antenna i hence is:

$$s_i(t) = h_i^b \sqrt{\Delta\sigma} h^f a(t) + L_i + n_i(t), \tag{5}$$

where $h_i^b = |h_i^b| e^{j\varphi_i^b}$ and $h^f = |h^f| e^{j\varphi^f}$ are the complex-valued backward and forward channel coefficient, respectively. The term $\Delta\sigma = |\Delta\sigma| e^{j2\varphi^{\Delta\sigma}}$ is the complex-valued normalised differential radar cross section and $L_i = |L_i| e^{j\varphi_i^{leak}}$ denotes the static and complex-valued carrier leakage. Finally, $n_i(t)$ is the complex-valued circularly symmetric white Gaussian noise with noise power spectral density N_0. Equivalently, we can reformulate Equation (5) to:

$$s_i(t) = h_i a(t) + L_i + n_i(t), \tag{6}$$

where $h_i = h^f \sqrt{\Delta\sigma} h_i^b$ is the channel coefficient of the equivalent dyadic channel from the transmitter of the reader to the tag and back to the i'th receive antenna of the reader [17]. Here also the modulation behaviour of the tag is modeled by the channel coefficient h (term $\sqrt{\Delta\sigma}$). By stacking the receive signals $s_i(t)$, channel coefficients h_i, carrier leakage L_i and noise components $n_i(t)$ of all N_R receive antennas into the $N_R \times 1$ vectors $\mathbf{s}(t)$, $\mathbf{h}$, $\mathbf{l}$ and $\mathbf{n}(t)$, respectively, Equation (6) is equivalently reformulated to:

$$\mathbf{s}(t) = \mathbf{h} a(t) + \mathbf{l} + \mathbf{n}(t). \tag{7}$$

If the tag absorbs energy, the tag absorb state $S_i^{(a)}$ is observed in the baseband I/Q plane of each antenna i ($a(t) = 0$ in Equation (6)). If the tag reflects energy however, the tag reflect state $S_i^{(r)}$ is identified in the I/Q baseband plane of each receive antenna i ($a(t) = 1$ in Equation (6)). While the tag absorb state $S_i^{(a)} = L_i$ corresponds to the carrier leakage at antenna i, the reflect state $S_i^{(r)} = L_i + h_i$ additionally includes the backscatter modulation. The location of the states in the I/Q baseband plane is arbitrary to the reader receiver, and depends on the extent of the carrier leakage L_i as well as on the channel coefficients h_i. The magnitude and phase of L_i and h_i depend on the spatial setup of reader and tag antennas as well as of the environmental scatterers, and on the transmitter to receiver decoupling scheme.

To verify our signal model, we recorded tag receive signals on our multiple antenna rapid prototyping system [18,19], and imported them into Matlab. The baseband receive constellations of the measurement are depicted in Figure 2. Obviously, the constellation on both antennas can be completely diverse, as phase and magnitude of both, the carrier leakage and the channel coefficient may be strongly distinct.

III. Direction of Arrival Estimation

Reviewing Equation (6), the subtraction of the carrier leakage from the receive signal at each antenna $s_i(t) - L_i = h_i a(t) + n_i(t)$, directly shows the channel coefficient modulated by the data, as demonstrated with the measurement data in Figure 3. In contrast to the carrier leakage, only the receive signal component from the tag carries information about its location. The angles φ_i of the constellation in the I/Q plane are composed of the forward channel phase shift φ^f, the phase shift due to the tag modulation $\varphi^{\Delta\sigma}$ and the backward channel phase shift φ_i^b:

$$\varphi_i \triangleq \varphi^f + \varphi^{\Delta\sigma} + \varphi_i^b. \tag{8}$$

As φ^f and $\varphi^{\Delta\sigma}$ affect both receive antenna constellations equally, a phase difference $\Delta\varphi = \varphi_i - \varphi_{i-1}$ in the constellation of the receive paths i and $i-1$ ($i \geq 2$) solely results from a distinct phase shift in the backward channels h_i^b and h_{i-1}^b. Assuming Line Of Sight (LOS) communication from the tag to the reader, the phase shift results from a different propagation delay from the tag to the various receive antennas. With a linear array of equidistant elements with spacing d and the tag-to-reader distance D much larger than the array size $D \gg (N-1)d$ (Figure 4), the phase difference between two neighbouring elements $\Delta\varphi$ is:

$$\Delta\varphi = kd\cos(\phi). \tag{9}$$

Here, $k = 2\pi/\lambda$ is the wave number, λ denotes the wavelength and ϕ is the Direction Of Arrival (DOA). The DOA is estimated by correlating the channel coefficients with the $N_R \times 1$ steering vector $\mathbf{t}(\phi)$,

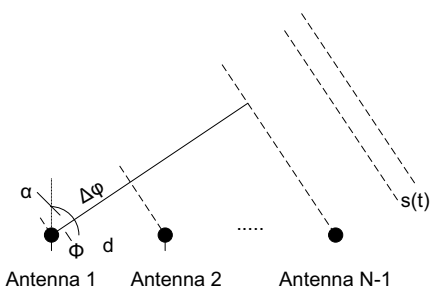

Figure 4: Localisation of RFID tag with multiple antennas.

whose i'th element is $e^{j(i-1)kd\cos(\phi)}$ [20]:

$$r(\phi) = \mathbf{h}^H \mathbf{t}(\phi)$$
$$= \sum_{i=1}^{N_R} h_i^* e^{jkd(i-1)\cos(\phi)}$$
$$\hat{\phi} = \arg\max_{\phi} |r(\phi)|. \quad (10)$$

The sum here essentially is the Discrete Time Fourier Transform (DTFT) of the channel coefficients h_i, with $\psi = kd\cos(\phi)$ denoting the spatial frequency. Consider h_i as the excitation of antenna i, then the DTFT is the array factor. Its maximum serves as the estimate for the DOA ϕ. Due to the above assumptions of LOS and $D \gg (N-1)d$ the path loss on all receive antennas is approximately equal $|h_i| \approx |h_j|$, thus distinct channel coefficients only differ in a phase shift.

In our experimental setup with only $N_R = 2$ receive antennas Equation (10) reduces to:

$$\hat{\phi} = \arg\max_{\phi} \left(e^{-j\varphi_1} + e^{-j\varphi_2} e^{jkd\cos(\phi)} \right), \quad (11)$$

$$-\varphi_1 = -\varphi_2 + kd\cos(\hat{\phi}), \quad (12)$$

$$\hat{\phi} = \arccos\left(\frac{\Delta\varphi}{kd}\right), \quad (13)$$

where Equation (12) results from Equation (11) with the argument, that for maximum magnitude the phases of both terms must be equal (Triangle Inequality).

The argument of the $\arccos(\cdot)$ term in Equation (13) must be in the range of -1 to 1, i.e. $\frac{\Delta\varphi}{kd} \in [-1, 1]$. If $d < \lambda/2$, only a single solution is possible. If $d > \lambda/2$ however, multiple solutions are possible, due to the 2π-periocity of $\Delta\varphi$, e.g. two possible solutions for $\lambda/2 < d < \lambda$. These solutions occur due to so-called grating lobes in the beam pattern [20, 21] for arrays with element spacing $d > \lambda/2$. However, there is only a single solution within the span $\phi \in [\arccos(\frac{\pi}{kd}), \arccos(\frac{-\pi}{kd})]$ for $\lambda/2 < d < \lambda$.

IV. Implementation

The above described algorithm is implemented on our dual receive antenna rapid prototyping system for RFID [18, 19]. The rapid prototyping system consists of a digital baseband hardware and analogue Radio Frequency (RF) frontends, supporting the UHF frequency domain. The digital baseband hardware is composed of a Digital Signal Processor (DSP), a Field Programmable Gate Array (FPGA), Digital to Analogue and Analogue to Digital Converters (DACs, ADCs). While the digital baseband hardware generates the transmit signal and detects and decodes the receive signal, the analogue frontend executes frequency up- and downconversion, filtering and amplification.

In order to estimate the DOA by Equation (13), the receiver requires knowledge about the carrier leakage L_i and the channel coefficient h_i at each antenna, which further allows the computation of φ_i as defined in Equation (8). The carrier leakage is estimated during a time period before the start of the uplink modulation, which is defined by T_1 in the standard of EPCglobal for UHF RFID [22]. The standard defines an idle time during this period (no backscatter modulation), hence the reader just receives the static carrier leakage, which is estimated as the temporal average of the receive signal during this period at each antenna i:

$$L_i = E\{s_i(t)\}_{T_1}. \quad (14)$$

With knowledge of the carrier leakage, the constellation is shifted to the origin, by subtracting the carrier leakage from the receive signal (compare with Figure 3). According to Equation (6), this shifted receive signal then is only composed of the tag receive signal and the noise. The tag reflects energy during the first bit of the preamble. Thus, this backscattered modulation signal during this first bit period $t1bit$ is proportional to the channel coefficient. Therefore, the channel coefficient is estimated as the temporal average of the receive signal with subtracted carrier leakage during this period:

$$h_i = E\{s_i(t) - L_i\}_{t1bit} \quad (15)$$

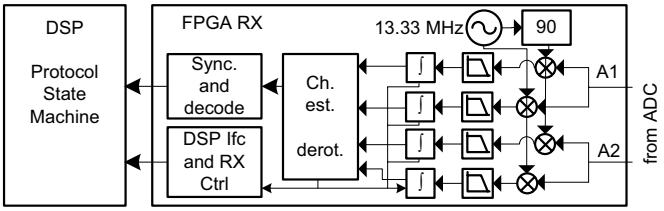

Figure 5: Implemented digital reciever architecture: the signal from the analogue frontends is captured at an intermediate frequency of 13.33 MHz. After digital down conversion and matched filtering, the channel is estimated and the phase shift is determined by a CORDIC algorithm.

A blockdiagram of the real-time digital (FPGA) receiver is shown in Figure 5. The interface to the RF frontend is realised by the ADC at an intermediate frequency of 13.33 MHz. This is one third of the FPGA and DAC / ADC clock frequency of 40 MHz, which facilitates the design of the digital sine and cosine generation. After the downconversion with low-pass filtering, a matched filter is applied to the receive sequences (denoted by the integration block in the blockdiagram of Figure 5). The subsequent finite state machine estimates the channel [23, 24] and detects the phase shift of the two receive constellations. The phase φ_i of the channel coefficient h_i is determined by applying a COrdinated Rotation Digital Integrated Circuit (CORDIC) algorithm with eight stages [25]. The constellation is rotated towards the real axis ($\varphi_i = 0$) in each CORDIC stage, with either a clockwise or counterclockwise rotation. By registering the clockwise or counterclockwise rotation direction, the receiver is capable to determine the angle φ_i and computes the phase shift $\Delta\varphi$. Eventually, the division and $\arccos(\cdot)$ operations of Equation (13) are computed on the DSP of the rapid prototyping system. Additionally, the two receive paths are combined as described in [23], and the combined signal is subsequently synchronised and decoded [26].

In constrast to the conventional single receive antenna or antenna switching receivers, this dual antenna receiver requires the duplication of the receive paths. Therefore two RF frontends, two ADCs and two individual digital receive chains are required. The duplication in the FPGA design requires two additional multipliers for the downconversion, while the filters are designed as moving average blocks, which do not consume any multipliers. Additionally, the channel estimation needs to be implemented for both receiver chains [23].

V. Experimental Evaluation

The following experimental evaluation results demonstrate the feasibility of DOA estimation in a scenario with low fading.

5.1 Measurement Setup

Figure 6 depicts the spatial measurement setup (also compare with [27] for the description of a similar experimental test scenario). The tag is moved at a y-position of zero meters in front of the reader antennas to distinct x-positions by means of a motor driven nylon cord. At each location, the tag is activated by a "Query" command from the reader, following the EPCglobal standard for passive UHF RFID [22]. The readout is repeated for 5×10^4 iterations. An average of φ_i is recorded at each position.

After the readouts at a certain location are completed, the procedure is repeated at the next position. The actualised x-spacing for the various positions of the measurements is 2 cm. The TX and RX antennas are positioned to minimise the carrier leakage in the receive paths.

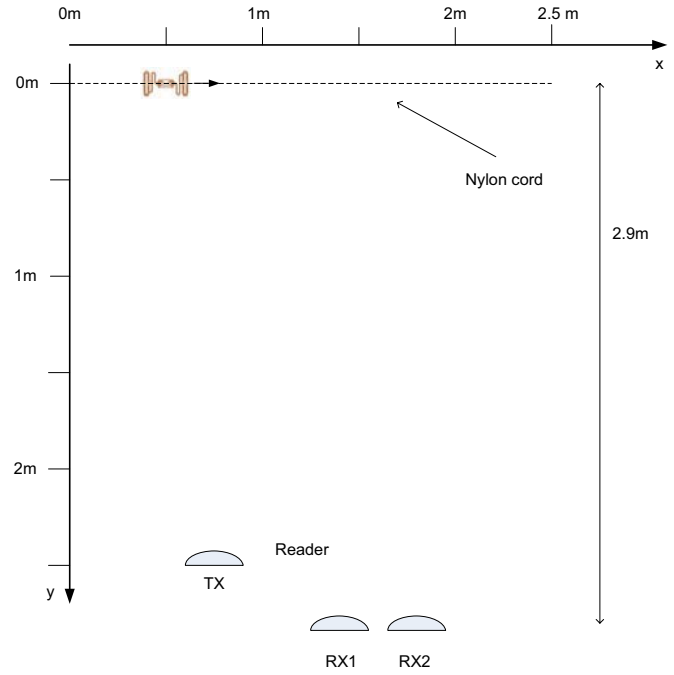

Figure 6: Measurement setup: the tag is moved on the nylon cord to positions with 0.02 m x-spacing and an y-position at zero meters. At each location, 50×10^4 measures are performed, and an average of the measured angle is computed. The antenna positions are: TX=(0.8m/2.5m), RX1=(1.4m/2.9m), RX2=(1.7m/2.9m).

This has been achieved by observing the carrier leakage in both receive paths on the oscilloscope, depending on the position of the RX antennas.

All antennas are commercially available RFID patch antennas. The employed transmit antenna has a gain of 9 dBi while the two receive antennas feature a gain of 8 dBi. The spacing between the two receive antennas is 30 cm, or 0.87λ for the corresponding frequency of 868 MHz. Thus, we in general expect two solutions for solving Equation (13). In the area $\phi \in [54.9°, 125.1°]$ however, only a single solution is obtained, which includes the measured area $\phi \in [77°, 118°]$, as depicted in Figure 6.

The measurement is conducted in a measurement room with almost no fading (quasi-anechoic room) for evaluation of the DOA estimation capabilities of the receiver. Hence, the only movement during the measurement is the tag itself, which is mounted on the electrically invisible nylon cord to avoid an influence on the measurement result due to the fixture of the tag. Additionally, only the antennas of the RFID reader are placed inside the measurement room, while the frontends and digital baseband hardware reside outside. The transmit power is set to 25.5 dBm.

The measurement is controlled by Matlab, which activates the rapid prototyping board via the Local Area Network (LAN) to read out the tag at a certain position for the 5×10^4 iterations, stores the results after completion, and triggers the tag movement to the neighbouring x-position, before the next readout is initiated. Throughout the measurement, a single tag was used [28].

5.2 Experimental Results

Figure 7 shows the experimental result of the direction of arrival estimation in terms of the incidence angle $\alpha = 90° - \phi$ (see Figure 4). The measurement is conducted in a measurement room with very low fading (quasi-anechoic), for a y-position of 0 m and variable x-position. The tracked $\Delta\varphi$ value results from a propagation delay to the two receive antennas, but also from a delay difference in the frontends (e.g. different cable lengths). Therefore, the DOA estimation is calibrated

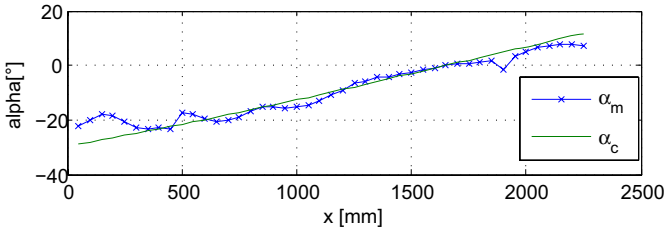

Figure 7: Experimental result of DOA estimation: $\alpha = 90 - \phi$: measured angle α_m and calculated angle α_c.

at $\alpha = 0°$ and subsequently the frontend delay is compensated.

The measured angle α_m is plotted versus the x-position in Figure 7, and is compared to the calculated angle $\alpha_c = \arctan \frac{x-x_0}{y_0-y}$, where x_0 and y_0 is the position of the receive antenna. At positions $x > 2.26$ m the tag is outside the coverage area of the transmit antenna of the reader. The maximum deviation from α_c is $10°$ on the very left side. This results form a very weak receive signal at these positions and from reflections from the wall close to the tag. The root of the averaged squared error over $N + 1 = \frac{x_{max}}{\Delta x} + 1 = \frac{226}{2} + 1 = 114$ positions $\bar{\epsilon}$ is shown to be 3.3°:

$$\bar{\epsilon} = \sqrt{\frac{1}{N+1} \sum_{x=0}^{N} (\alpha_m(x) - \alpha_c(x))^2}. \tag{16}$$

The result demonstrates that a DOA estimation even with only two receive antennas is feasible in an environment with a strong LOS component.

VI. Conclusion

In this paper we propose to enrich the functionality of multiple receive antenna RFID readers with direction of arrival estimation capabilities. A model for signal constellations at multiple receive antenna reader receivers is proposed. Based on that model, we develop the DOA estimation algorithm for passive RFID. The algorithm is implemented on our rapid prototyping platform for RFID, and implementation details are presented. Additionally, the paper presents experimental evaluation results, which demonstrate that an DOA estimation in an environment with low fading is feasible with two receive antennas. The root of the averaged squared error over multiple positions is shown to be 3.3.

Acknowledgment

This work has been funded by the Christian Doppler Laboratory for Wireless Technologies for Sustainable Mobility, the Federal Ministry of Economy, Family and Youth and the National Foundation for Research, Technology and Development of Austria. The authors thank Christoph Mecklenbräuker for his valueable support and our industrial partner Infineon for enabling that work.

References

[1] M. Kim and N. Y. Chong. Direction sensing RFID reader for mobile robot navigation. *IEEE Transactions on Automation Science and Engineering*, 6(1):44–54, Jan. 2009.

[2] L. M. Ni, Y. Liu, Y. C. Lau, and A. P. Patil. LANDMARC: indoor location sensing using active RFID. *Wireless Networks*, 10:701–710, 2004. Springer Netherlands.

[3] G. Jin, X. Lu, and M. Park. An indoor localization mechanism using active RFID tag. In *Proc. of the IEEE International Conference on Sensor Networks, Ubiquitous, and Trustworthy Computing.*, Jun. 2006.

[4] S. Han, H. Lim, and J. Lee. An efficient localization scheme for a differential-driving moblie robot based RFID system. *IEEE Transactions on Industrial Electronics*, 54(6):3362–3369, Dec. 2007.

[5] Y. Zhang, M. G. Amin, and S. Kaushik. Localization and tracking of passive RFID tags based on direction estimation. *International Journal of Antennas and Propagation*, 2007, 2007.

[6] M. J. Abedin and A. S. Mohan. Use of smart antennas for the localization of RFID reader. In *Proc. of the Asia Pacific Microwave Conference*, pages 1036–1039, 2009.

[7] Z. Tongliang, W. Feng, T. Hui, and C. Jianming. The performance analysis using multiple beams for RFID warehouse management system. In *Proc. of the IEEE 24th International Conference on Advanced Information Netwoking and Applications Workshop*, pages 567–570, 2010.

[8] P. Salonen, M. Keskilammi, L. Sydanheimo, and M. Kivikoski. An intelligent 2.45 GHz beam-scanning array for modern RFID reader. In *Proc. of the IEEE International Conference on Phased Array Systems and Technology*, 2000.

[9] P. V. Nikitin, R. Martinez, S. Ramamurthy, H. Leland, G. Spiess, and K. V. S. Rao. Phase based spatial identification of UHF RFID tags. In *Proc. of the IEEE International Conference on RFID*, Apr. 2010.

[10] C. Hekimian-Williams, B. Grant, X. Liu, Z. Zhang, and P. Kumar. Accurate localization of RFID tags using phase difference. In *Proc. of the IEEE International Conference on RFID*, Apr. 2010.

[11] M. Y. W. Chia, K. C. M. Ang, K. L. Lee, and S. W. Leong. A smart beam steering RFID interrogator for passive tags in item level tagging applications. In *Proc. of the IEEE MTT-S International Microwave Symposium Digest*, 2008.

[12] M. Y. W. Chia, P. Y. Chee, W. F. Loke, J. K. Yin, K. C. M. Ang, S. W. Leong, K. L. Chee, and A. A. L. Peh. Electronic beam-steering IC for multimode and multiband RFID. *IEEE Transactions on Microwave Theory and Techniques*, 57(5):1310–1319, May 2009.

[13] D. Arnitz, K. Witrisal, and U. Muehlmann. Multifrequency continuous-wave radar approach to ranging in passive UHF RFID. *IEEE Transactions on Microwave Theory and Techniques*, 57(5), May 2009.

[14] L. W. Mayer, R. Langwieser, and A. L. Scholtz. Evaluation of passive carrier-suppression techniques for UHF RFID systems. In *Proc. of the IEEE MTT-S International Microwave Workshop on Wireless Sensing, Local Positioning and RFID*, Cavtat, Croatia, Sept. 2009.

[15] R. Langwieser, G. Lasser, C. Angerer, M. Fischer, and A.L. Scholtz. Active carrier compensation for a multi-antenna RFID frontend. In *Proc. of the IEEE International Microwave Symposium*, Anaheim, USA, May 2010.

[16] P. V. Nikitin, K. V. S. Rao, and R. D. Martinez. Differential RCS of RFID tag. *Electronic Letters*, 43(8):431–432, Apr. 2007.

[17] J. D. Griffin and G. D. Durgin. Gains for RF tags using multiple antennas. *IEEE Transaction on Antennas and Propagation*, 56(2):563–570, Feb. 2008.

[18] R. Langwieser, C. Angerer, and A. L. Scholtz. A UHF frontend for MIMO applications in RFID. In *Proc. of the 2010 IEEE Radio and Wireless Symposium*, New Orleans, USA, January 2010.

[19] C. Angerer, M. Holzer, B. Knerr, and M. Rupp. A flexible dual frequency testbed for RFID. In *Proc. of the 4th International Conference on Testbeds and Research Infrastructures for the Development of Networks & Communities*, Innsbruck, Austria, 2008.

[20] H. L. Van Trees. *Optimum Array Processing*. Wiley & Sons New York, 2002.

[21] C. Balanis. *Antenna Theory: Analysis and Design*. John Wiley, 1997.

[22] EPCGlobal. EPC Radio-Frequency Identity Protocols Class-1 Generation-2 UHF RFID, Oct. 2008. Version 1.2.0, http://www.epcglobalinc.org.

[23] C. Angerer, R. Langwieser, G. Maier, and M. Rupp. Maximal ratio combining receivers for dual antenna RFID readers. In *Proc. of the IEEE MTT-S International Microwave Workshop Series on Wireless Sensing, Local Positioning and RFID*, Cavtat, Croatia, Sept. 2009.

[24] C. Angerer. A digital receiver architecture for RFID readers. In *Proc. of the IEEE 3rd International Symposium on Industrial Embedded Systems*, pages 97–102, Montpellier, France, Jun. 2008.

[25] J. E. Volder. The CORDIC trigonometric computing technique. *IRE Transactions on Electronic Computers*, pages 330–334, Sept. 1959.

[26] C. Angerer and M. Rupp. Advanced synchronisation and decoding in RFID reader receivers. In *Proc. of the IEEE Radio and Wireless Symposium*, San Diego, USA, Jan. 2009.

[27] C. Angerer, R. Langwieser, and M. Rupp. Experimental performance evaluation of dual antenna diversity receivers for RFID readers. In *Proc. of the Third International EURASIP Workshop on RFID Technology*, Spain, Sept. 2010.

[28] UPM Raflatac, RFID. UPM raflatec dogbone, Feb. 2002. available at:"www.upmraflatac.com".